BABAR-PUB-06/017 SLAC-PUB-11850

Search for the decay $B^0 \to a_1^\pm \rho^\mp$

B. Aubert,[1] R. Barate,[1] M. Bona,[1] D. Boutigny,[1] F. Couderc,[1] Y. Karyotakis,[1] J. P. Lees,[1] V. Poireau,[1]
V. Tisserand,[1] A. Zghiche,[1] E. Grauges,[2] A. Palano,[3] M. Pappagallo,[3] J. C. Chen,[4] N. D. Qi,[4] G. Rong,[4] P. Wang,[4]
Y. S. Zhu,[4] G. Eigen,[5] I. Ofte,[5] B. Stugu,[5] G. S. Abrams,[6] M. Battaglia,[6] D. N. Brown,[6] J. Button-Shafer,[6]
R. N. Cahn,[6] E. Charles,[6] C. T. Day,[6] M. S. Gill,[6] Y. Groysman,[6] R. G. Jacobsen,[6] J. A. Kadyk,[6] L. T. Kerth,[6]
Yu. G. Kolomensky,[6] G. Kukartsev,[6] G. Lynch,[6] L. M. Mir,[6] P. J. Oddone,[6] T. J. Orimoto,[6] M. Pripstein,[6]
N. A. Roe,[6] M. T. Ronan,[6] W. A. Wenzel,[6] M. Barrett,[7] K. E. Ford,[7] T. J. Harrison,[7] A. J. Hart,[7] C. M. Hawkes,[7]
S. E. Morgan,[7] A. T. Watson,[7] K. Goetzen,[8] T. Held,[8] H. Koch,[8] B. Lewandowski,[8] M. Pelizaeus,[8] K. Peters,[8]
T. Schroeder,[8] M. Steinke,[8] J. T. Boyd,[9] J. P. Burke,[9] W. N. Cottingham,[9] D. Walker,[9] T. Cuhadar-Donszelmann,[10]
B. G. Fulsom,[10] C. Hearty,[10] N. S. Knecht,[10] T. S. Mattison,[10] J. A. McKenna,[10] A. Khan,[11] P. Kyberd,[11]
M. Saleem,[11] L. Teodorescu,[11] V. E. Blinov,[12] A. D. Bukin,[12] V. P. Druzhinin,[12] V. B. Golubev,[12] A. P. Onuchin,[12]
S. I. Serednyakov,[12] Yu. I. Skovpen,[12] E. P. Solodov,[12] K. Yu Todyshev,[12] D. S. Best,[13] M. Bondioli,[13]
M. Bruinsma,[13] M. Chao,[13] S. Curry,[13] I. Eschrich,[13] D. Kirkby,[13] A. J. Lankford,[13] P. Lund,[13] M. Mandelkern,[13]
R. K. Mommsen,[13] W. Roethel,[13] D. P. Stoker,[13] S. Abachi,[14] C. Buchanan,[14] S. D. Foulkes,[15] J. W. Gary,[15]
O. Long,[15] B. C. Shen,[15] K. Wang,[15] L. Zhang,[15] H. K. Hadavand,[16] E. J. Hill,[16] H. P. Paar,[16] S. Rahatlou,[16]
V. Sharma,[16] J. W. Berryhill,[17] C. Campagnari,[17] A. Cunha,[17] B. Dahmes,[17] T. M. Hong,[17] D. Kovalskyi,[17]
J. D. Richman,[17] T. W. Beck,[18] A. M. Eisner,[18] C. J. Flacco,[18] C. A. Heusch,[18] J. Kroseberg,[18] W. S. Lockman,[18]
G. Nesom,[18] T. Schalk,[18] B. A. Schumm,[18] A. Seiden,[18] P. Spradlin,[18] D. C. Williams,[18] M. G. Wilson,[18]
J. Albert,[19] E. Chen,[19] A. Dvoretskii,[19] D. G. Hitlin,[19] I. Narsky,[19] T. Piatenko,[19] F. C. Porter,[19] A. Ryd,[19]
A. Samuel,[19] R. Andreassen,[20] G. Mancinelli,[20] B. T. Meadows,[20] M. D. Sokoloff,[20] F. Blanc,[21] P. C. Bloom,[21]
S. Chen,[21] W. T. Ford,[21] J. F. Hirschauer,[21] A. Kreisel,[21] U. Nauenberg,[21] A. Olivas,[21] W. O. Ruddick,[21]
J. G. Smith,[21] K. A. Ulmer,[21] S. R. Wagner,[21] J. Zhang,[21] A. Chen,[22] E. A. Eckhart,[22] A. Soffer,[22] W. H. Toki,[22]
R. J. Wilson,[22] F. Winklmeier,[22] Q. Zeng,[22] D. D. Altenburg,[23] E. Feltresi,[23] A. Hauke,[23] H. Jasper,[23] B. Spaan,[23]
T. Brandt,[24] V. Klose,[24] H. M. Lacker,[24] W. F. Mader,[24] R. Nogowski,[24] A. Petzold,[24] J. Schubert,[24]
K. R. Schubert,[24] R. Schwierz,[24] J. E. Sundermann,[24] A. Volk,[24] D. Bernard,[25] G. R. Bonneaud,[25] P. Grenier,[25, *]
E. Latour,[25] Ch. Thiebaux,[25] M. Verderi,[25] D. J. Bard,[26] P. J. Clark,[26] W. Gradl,[26] F. Muheim,[26] S. Playfer,[26]
A. I. Robertson,[26] Y. Xie,[26] M. Andreotti,[27] D. Bettoni,[27] C. Bozzi,[27] R. Calabrese,[27] G. Cibinetto,[27] E. Luppi,[27]
M. Negrini,[27] A. Petrella,[27] L. Piemontese,[27] E. Prencipe,[27] F. Anulli,[28] R. Baldini-Ferroli,[28] A. Calcaterra,[28]
R. de Sangro,[28] G. Finocchiaro,[28] S. Pacetti,[28] P. Patteri,[28] I. M. Peruzzi,[28, †] M. Piccolo,[28] M. Rama,[28]
A. Zallo,[28] A. Buzzo,[29] R. Capra,[29] R. Contri,[29] M. Lo Vetere,[29] M. M. Macri,[29] M. R. Monge,[29] S. Passaggio,[29]
C. Patrignani,[29] E. Robutti,[29] A. Santroni,[29] S. Tosi,[29] G. Brandenburg,[30] K. S. Chaisanguanthum,[30] M. Morii,[30]
J. Wu,[30] R. S. Dubitzky,[31] J. Marks,[31] S. Schenk,[31] U. Uwer,[31] W. Bhimji,[32] D. A. Bowerman,[32] P. D. Dauncey,[32]
U. Egede,[32] R. L. Flack,[32] J. R. Gaillard,[32] J .A. Nash,[32] M. B. Nikolich,[32] W. Panduro Vazquez,[32] X. Chai,[33]
M. J. Charles,[33] U. Mallik,[33] N. T. Meyer,[33] V. Ziegler,[33] J. Cochran,[34] H. B. Crawley,[34] L. Dong,[34] V. Eyges,[34]
W. T. Meyer,[34] S. Prell,[34] E. I. Rosenberg,[34] A. E. Rubin,[34] A. V. Gritsan,[35] M. Fritsch,[36] G. Schott,[36]
N. Arnaud,[37] M. Davier,[37] G. Grosdidier,[37] A. Höcker,[37] F. Le Diberder,[37] V. Lepeltier,[37] A. M. Lutz,[37]
A. Oyanguren,[37] S. Pruvot,[37] S. Rodier,[37] P. Roudeau,[37] M. H. Schune,[37] A. Stocchi,[37] W. F. Wang,[37]
G. Wormser,[37] C. H. Cheng,[38] D. J. Lange,[38] D. M. Wright,[38] C. A. Chavez,[39] I. J. Forster,[39] J. R. Fry,[39]
E. Gabathuler,[39] R. Gamet,[39] K. A. George,[39] D. E. Hutchcroft,[39] D. J. Payne,[39] K. C. Schofield,[39]
C. Touramanis,[39] A. J. Bevan,[40] F. Di Lodovico,[40] W. Menges,[40] R. Sacco,[40] C. L. Brown,[41] G. Cowan,[41]
H. U. Flaecher,[41] D. A. Hopkins,[41] P. S. Jackson,[41] T. R. McMahon,[41] S. Ricciardi,[41] F. Salvatore,[41] D. N. Brown,[42]
C. L. Davis,[42] J. Allison,[43] N. R. Barlow,[43] R. J. Barlow,[43] Y. M. Chia,[43] C. L. Edgar,[43] M. P. Kelly,[43]
G. D. Lafferty,[43] M. T. Naisbit,[43] J. C. Williams,[43] J. I. Yi,[43] C. Chen,[44] W. D. Hulsbergen,[44] A. Jawahery,[44]
C. K. Lae,[44] D. A. Roberts,[44] G. Simi,[44] G. Blaylock,[45] C. Dallapiccola,[45] S. S. Hertzbach,[45] X. Li,[45] T. B. Moore,[45]
S. Saremi,[45] H. Staengle,[45] S. Y. Willocq,[45] R. Cowan,[46] K. Koeneke,[46] G. Sciolla,[46] S. J. Sekula,[46] M. Spitznagel,[46]
F. Taylor,[46] R. K. Yamamoto,[46] H. Kim,[47] P. M. Patel,[47] C. T. Potter,[47] S. H. Robertson,[47] A. Lazzaro,[48]
V. Lombardo,[48] F. Palombo,[48] J. M. Bauer,[49] L. Cremaldi,[49] V. Eschenburg,[49] R. Godang,[49] R. Kroeger,[49]
J. Reidy,[49] D. A. Sanders,[49] D. J. Summers,[49] H. W. Zhao,[49] S. Brunet,[50] D. Côté,[50] M. Simard,[50] P. Taras,[50]
F. B. Viaud,[50] H. Nicholson,[51] N. Cavallo,[52, ‡] G. De Nardo,[52] D. del Re,[52] F. Fabozzi,[52, ‡] C. Gatto,[52] L. Lista,[52]

D. Monorchio,[52] P. Paolucci,[52] D. Piccolo,[52] C. Sciacca,[52] M. Baak,[53] H. Bulten,[53] G. Raven,[53] H. L. Snoek,[53] C. P. Jessop,[54] J. M. LoSecco,[54] T. Allmendinger,[55] G. Benelli,[55] K. K. Gan,[55] K. Honscheid,[55] D. Hufnagel,[55] P. D. Jackson,[55] H. Kagan,[55] R. Kass,[55] T. Pulliam,[55] A. M. Rahimi,[55] R. Ter-Antonyan,[55] Q. K. Wong,[55] N. L. Blount,[56] J. Brau,[56] R. Frey,[56] O. Igonkina,[56] M. Lu,[56] R. Rahmat,[56] N. B. Sinev,[56] D. Strom,[56] J. Strube,[56] E. Torrence,[56] F. Galeazzi,[57] A. Gaz,[57] M. Margoni,[57] M. Morandin,[57] A. Pompili,[57] M. Posocco,[57] M. Rotondo,[57] F. Simonetto,[57] R. Stroili,[57] C. Voci,[57] M. Benayoun,[58] J. Chauveau,[58] P. David,[58] L. Del Buono,[58] Ch. de la Vaissière,[58] O. Hamon,[58] B. L. Hartfiel,[58] M. J. J. John,[58] Ph. Leruste,[58] J. Malclès,[58] J. Ocariz,[58] L. Roos,[58] G. Therin,[58] P. K. Behera,[59] L. Gladney,[59] J. Panetta,[59] M. Biasini,[60] R. Covarelli,[60] M. Pioppi,[60] C. Angelini,[61] G. Batignani,[61] S. Bettarini,[61] F. Bucci,[61] G. Calderini,[61] M. Carpinelli,[61] R. Cenci,[61] F. Forti,[61] M. A. Giorgi,[61] A. Lusiani,[61] G. Marchiori,[61] M. A. Mazur,[61] M. Morganti,[61] N. Neri,[61] E. Paoloni,[61] G. Rizzo,[61] J. Walsh,[61] M. Haire,[62] D. Judd,[62] D. E. Wagoner,[62] J. Biesiada,[63] N. Danielson,[63] P. Elmer,[63] Y. P. Lau,[63] C. Lu,[63] J. Olsen,[63] A. J. S. Smith,[63] A. V. Telnov,[63] F. Bellini,[64] G. Cavoto,[64] A. D'Orazio,[64] E. Di Marco,[64] R. Faccini,[64] F. Ferrarotto,[64] F. Ferroni,[64] M. Gaspero,[64] L. Li Gioi,[64] M. A. Mazzoni,[64] S. Morganti,[64] G. Piredda,[64] F. Polci,[64] F. Safai Tehrani,[64] C. Voena,[64] M. Ebert,[65] H. Schröder,[65] R. Waldi,[65] T. Adye,[66] N. De Groot,[66] B. Franek,[66] E. O. Olaiya,[66] F. F. Wilson,[66] S. Emery,[67] A. Gaidot,[67] S. F. Ganzhur,[67] G. Hamel de Monchenault,[67] W. Kozanecki,[67] M. Legendre,[67] B. Mayer,[67] G. Vasseur,[67] Ch. Yèche,[67] M. Zito,[67] W. Park,[68] M. V. Purohit,[68] A. W. Weidemann,[68] J. R. Wilson,[68] M. T. Allen,[69] D. Aston,[69] R. Bartoldus,[69] P. Bechtle,[69] N. Berger,[69] A. M. Boyarski,[69] R. Claus,[69] J. P. Coleman,[69] M. R. Convery,[69] M. Cristinziani,[69] J. C. Dingfelder,[69] D. Dong,[69] J. Dorfan,[69] G. P. Dubois-Felsmann,[69] D. Dujmic,[69] W. Dunwoodie,[69] R. C. Field,[69] T. Glanzman,[69] S. J. Gowdy,[69] M. T. Graham,[69] V. Halyo,[69] C. Hast,[69] T. Hryn'ova,[69] W. R. Innes,[69] M. H. Kelsey,[69] P. Kim,[69] M. L. Kocian,[69] D. W. G. S. Leith,[69] S. Li,[69] J. Libby,[69] S. Luitz,[69] V. Luth,[69] H. L. Lynch,[69] D. B. MacFarlane,[69] H. Marsiske,[69] R. Messner,[69] D. R. Muller,[69] C. P. O'Grady,[69] V. E. Ozcan,[69] A. Perazzo,[69] M. Perl,[69] B. N. Ratcliff,[69] A. Roodman,[69] A. A. Salnikov,[69] R. H. Schindler,[69] J. Schwiening,[69] A. Snyder,[69] J. Stelzer,[69] D. Su,[69] M. K. Sullivan,[69] K. Suzuki,[69] S. K. Swain,[69] J. M. Thompson,[69] J. Va'vra,[69] N. van Bakel,[69] M. Weaver,[69] A. J. R. Weinstein,[69] W. J. Wisniewski,[69] M. Wittgen,[69] D. H. Wright,[69] A. K. Yarritu,[69] K. Yi,[69] C. C. Young,[69] P. R. Burchat,[70] A. J. Edwards,[70] S. A. Majewski,[70] B. A. Petersen,[70] C. Roat,[70] L. Wilden,[70] S. Ahmed,[71] M. S. Alam,[71] R. Bula,[71] J. A. Ernst,[71] V. Jain,[71] B. Pan,[71] M. A. Saeed,[71] F. R. Wappler,[71] S. B. Zain,[71] W. Bugg,[72] M. Krishnamurthy,[72] S. M. Spanier,[72] R. Eckmann,[73] J. L. Ritchie,[73] A. Satpathy,[73] C. J. Schilling,[73] R. F. Schwitters,[73] J. M. Izen,[74] I. Kitayama,[74] X. C. Lou,[74] S. Ye,[74] F. Bianchi,[75] F. Gallo,[75] D. Gamba,[75] M. Bomben,[76] L. Bosisio,[76] C. Cartaro,[76] F. Cossutti,[76] G. Della Ricca,[76] S. Dittongo,[76] S. Grancagnolo,[76] L. Lanceri,[76] L. Vitale,[76] V. Azzolini,[77] F. Martinez-Vidal,[77] Sw. Banerjee,[78] B. Bhuyan,[78] C. M. Brown,[78] D. Fortin,[78] K. Hamano,[78] R. Kowalewski,[78] I. M. Nugent,[78] J. M. Roney,[78] R. J. Sobie,[78] J. J. Back,[79] P. F. Harrison,[79] T. E. Latham,[79] G. B. Mohanty,[79] H. R. Band,[80] X. Chen,[80] B. Cheng,[80] S. Dasu,[80] M. Datta,[80] A. M. Eichenbaum,[80] K. T. Flood,[80] J. J. Hollar,[80] J. R. Johnson,[80] P. E. Kutter,[80] H. Li,[80] R. Liu,[80] B. Mellado,[80] A. Mihalyi,[80] A. K. Mohapatra,[80] Y. Pan,[80] M. Pierini,[80] R. Prepost,[80] P. Tan,[80] S. L. Wu,[80] Z. Yu,[80] and H. Neal[81]

(The *BABAR* Collaboration)

[1]*Laboratoire de Physique des Particules, F-74941 Annecy-le-Vieux, France*
[2]*Universitat de Barcelona, Facultat de Fisica Dept. ECM, E-08028 Barcelona, Spain*
[3]*Università di Bari, Dipartimento di Fisica and INFN, I-70126 Bari, Italy*
[4]*Institute of High Energy Physics, Beijing 100039, China*
[5]*University of Bergen, Institute of Physics, N-5007 Bergen, Norway*
[6]*Lawrence Berkeley National Laboratory and University of California, Berkeley, California 94720, USA*
[7]*University of Birmingham, Birmingham, B15 2TT, United Kingdom*
[8]*Ruhr Universität Bochum, Institut für Experimentalphysik 1, D-44780 Bochum, Germany*
[9]*University of Bristol, Bristol BS8 1TL, United Kingdom*
[10]*University of British Columbia, Vancouver, British Columbia, Canada V6T 1Z1*
[11]*Brunel University, Uxbridge, Middlesex UB8 3PH, United Kingdom*
[12]*Budker Institute of Nuclear Physics, Novosibirsk 630090, Russia*
[13]*University of California at Irvine, Irvine, California 92697, USA*
[14]*University of California at Los Angeles, Los Angeles, California 90024, USA*
[15]*University of California at Riverside, Riverside, California 92521, USA*
[16]*University of California at San Diego, La Jolla, California 92093, USA*
[17]*University of California at Santa Barbara, Santa Barbara, California 93106, USA*
[18]*University of California at Santa Cruz, Institute for Particle Physics, Santa Cruz, California 95064, USA*
[19]*California Institute of Technology, Pasadena, California 91125, USA*

[20]University of Cincinnati, Cincinnati, Ohio 45221, USA
[21]University of Colorado, Boulder, Colorado 80309, USA
[22]Colorado State University, Fort Collins, Colorado 80523, USA
[23]Universität Dortmund, Institut für Physik, D-44221 Dortmund, Germany
[24]Technische Universität Dresden, Institut für Kern- und Teilchenphysik, D-01062 Dresden, Germany
[25]Ecole Polytechnique, LLR, F-91128 Palaiseau, France
[26]University of Edinburgh, Edinburgh EH9 3JZ, United Kingdom
[27]Università di Ferrara, Dipartimento di Fisica and INFN, I-44100 Ferrara, Italy
[28]Laboratori Nazionali di Frascati dell'INFN, I-00044 Frascati, Italy
[29]Università di Genova, Dipartimento di Fisica and INFN, I-16146 Genova, Italy
[30]Harvard University, Cambridge, Massachusetts 02138, USA
[31]Universität Heidelberg, Physikalisches Institut, Philosophenweg 12, D-69120 Heidelberg, Germany
[32]Imperial College London, London, SW7 2AZ, United Kingdom
[33]University of Iowa, Iowa City, Iowa 52242, USA
[34]Iowa State University, Ames, Iowa 50011-3160, USA
[35]Johns Hopkins University, Baltimore, Maryland 21218, USA
[36]Universität Karlsruhe, Institut für Experimentelle Kernphysik, D-76021 Karlsruhe, Germany
[37]Laboratoire de l'Accélérateur Linéaire, IN2P3-CNRS et Université Paris-Sud 11,
Centre Scientifique d'Orsay, B.P. 34, F-91898 ORSAY Cedex, France
[38]Lawrence Livermore National Laboratory, Livermore, California 94550, USA
[39]University of Liverpool, Liverpool L69 7ZE, United Kingdom
[40]Queen Mary, University of London, E1 4NS, United Kingdom
[41]University of London, Royal Holloway and Bedford New College, Egham, Surrey TW20 0EX, United Kingdom
[42]University of Louisville, Louisville, Kentucky 40292, USA
[43]University of Manchester, Manchester M13 9PL, United Kingdom
[44]University of Maryland, College Park, Maryland 20742, USA
[45]University of Massachusetts, Amherst, Massachusetts 01003, USA
[46]Massachusetts Institute of Technology, Laboratory for Nuclear Science, Cambridge, Massachusetts 02139, USA
[47]McGill University, Montréal, Québec, Canada H3A 2T8
[48]Università di Milano, Dipartimento di Fisica and INFN, I-20133 Milano, Italy
[49]University of Mississippi, University, Mississippi 38677, USA
[50]Université de Montréal, Physique des Particules, Montréal, Québec, Canada H3C 3J7
[51]Mount Holyoke College, South Hadley, Massachusetts 01075, USA
[52]Università di Napoli Federico II, Dipartimento di Scienze Fisiche and INFN, I-80126, Napoli, Italy
[53]NIKHEF, National Institute for Nuclear Physics and High Energy Physics, NL-1009 DB Amsterdam, The Netherlands
[54]University of Notre Dame, Notre Dame, Indiana 46556, USA
[55]Ohio State University, Columbus, Ohio 43210, USA
[56]University of Oregon, Eugene, Oregon 97403, USA
[57]Università di Padova, Dipartimento di Fisica and INFN, I-35131 Padova, Italy
[58]Universités Paris VI et VII, Laboratoire de Physique Nucléaire et de Hautes Energies, F-75252 Paris, France
[59]University of Pennsylvania, Philadelphia, Pennsylvania 19104, USA
[60]Università di Perugia, Dipartimento di Fisica and INFN, I-06100 Perugia, Italy
[61]Università di Pisa, Dipartimento di Fisica, Scuola Normale Superiore and INFN, I-56127 Pisa, Italy
[62]Prairie View A&M University, Prairie View, Texas 77446, USA
[63]Princeton University, Princeton, New Jersey 08544, USA
[64]Università di Roma La Sapienza, Dipartimento di Fisica and INFN, I-00185 Roma, Italy
[65]Universität Rostock, D-18051 Rostock, Germany
[66]Rutherford Appleton Laboratory, Chilton, Didcot, Oxon, OX11 0QX, United Kingdom
[67]DSM/Dapnia, CEA/Saclay, F-91191 Gif-sur-Yvette, France
[68]University of South Carolina, Columbia, South Carolina 29208, USA
[69]Stanford Linear Accelerator Center, Stanford, California 94309, USA
[70]Stanford University, Stanford, California 94305-4060, USA
[71]State University of New York, Albany, New York 12222, USA
[72]University of Tennessee, Knoxville, Tennessee 37996, USA
[73]University of Texas at Austin, Austin, Texas 78712, USA
[74]University of Texas at Dallas, Richardson, Texas 75083, USA
[75]Università di Torino, Dipartimento di Fisica Sperimentale and INFN, I-10125 Torino, Italy
[76]Università di Trieste, Dipartimento di Fisica and INFN, I-34127 Trieste, Italy
[77]IFIC, Universitat de Valencia-CSIC, E-46071 Valencia, Spain
[78]University of Victoria, Victoria, British Columbia, Canada V8W 3P6
[79]Department of Physics, University of Warwick, Coventry CV4 7AL, United Kingdom
[80]University of Wisconsin, Madison, Wisconsin 53706, USA
[81]Yale University, New Haven, Connecticut 06511, USA

(Dated: June 25, 2018)

We present a search for the rare B-meson decay $B^0 \to a_1^{\pm}\rho^{\mp}$ with $a_1^{\pm} \to \pi^+\pi^-\pi^{\pm}$. We use $(110 \pm 1.2) \times 10^6$ $\Upsilon(4S) \to B\overline{B}$ decays collected with the *BABAR* detector at the PEP-II asymmetric-energy B Factory at SLAC. We obtain an upper limit of $30{\times}10^{-6}$ (90% C.L.) for the branching fraction product $\mathcal{B}(B^0 \to a_1^{\pm}\rho^{\mp})\mathcal{B}(a_1^{\pm} \to \pi^+\pi^-\pi^{\pm})$, where we assume that the $a_1^{\pm}$ decays exclusively to $\rho^0\pi^{\pm}$.

PACS numbers: 13.25.Hw, 12.15.Hh, 11.30.Er

In the Standard Model, *CP*-violating effects in the B-meson system arise from a single phase in the Cabibbo-Kobayashi-Maskawa (CKM) quark-mixing matrix [1]. The decay $B^0 \to a_1^{\pm}\rho^{\mp}$ proceeds via a $\overline{b} \to u\overline{u}d$ transition [2], and interference between direct decay and decay after $B^0\overline{B}^0$ mixing results in a time-dependent decay-rate asymmetry that is sensitive to the angle $\alpha \equiv \arg[-V_{td}V_{tb}^*/V_{ud}V_{ub}^*]$ [3] in the unitarity triangle of the CKM matrix. An additional motivation for studying $B^0 \to a_1^{\pm}\rho^{\mp}$ is that this is a significant background to $B \to \rho\rho$ decays, e.g. [4–8], which currently provide the most accurate measurement of α. The ARGUS experiment previously searched for the decay $B^0 \to a_1^{\pm}\rho^{\mp}$, which resulted in an upper limit of $\mathcal{B}(B^0 \to a_1^{\pm}\rho^{\mp}) < 3.4 \times 10^{-3}$ (90% C.L.) [9]. This paper presents the result of a search for $B^0 \to a_1^{\pm}\rho^{\mp}$ with $a_1^{\pm} \to \pi^+\pi^-\pi^{\pm}$, where we assume that the $a_1^{\pm}$ decays exclusively to $\rho^0\pi^{\pm}$. A theoretical prediction of the branching fraction $\mathcal{B}(B^0 \to a_1^{\pm}\rho^{\mp})\mathcal{B}(a_1^{\pm} \to (3\pi)^{\pm})$ has been made by Bauer, Stech and Wirbel [10] within the framework of the factorization model. They predict a value of $43{\times}10^{-6}$, assuming $|V_{ub}/V_{cb}| = 0.08$.

The data used in this analysis were collected with the *BABAR* detector at the PEP-II asymmetric-energy B Factory at SLAC during the years 2003-2004. This represents a total integrated luminosity of 100 fb^{-1} taken at the Υ(4S) resonance (on-peak), corresponding to a sample of 110 $\pm$ 1.2 million $B\overline{B}$ pairs. An additional 21.6 fb^{-1} of data, collected at approximately 40 MeV below the Υ(4S) resonance (off-peak), were used to study background from $e^+e^- \to q\overline{q}$ $(q = u, d, s, c)$ continuum events.

The *BABAR* detector is described in detail elsewhere [11]. Surrounding the interaction point is a silicon vertex tracker (SVT) with 5 double-sided layers which measures the impact parameters of charged particle tracks in both the plane transverse to, and along the beam direction. A 40 layer drift chamber (DCH) surrounds the SVT and provides measurements of the transverse momenta for charged particles. Both the SVT and the DCH operate in the magnetic field of a 1.5 T solenoid. Charged hadron identification is achieved through measurements of particle energy-loss in the tracking system and the Cherenkov angle obtained from a detector of internally reflected Cherenkov light. A CsI(Tl) electromagnetic calorimeter (EMC) provides photon detection, electron identification, and π^0 reconstruction. Finally, the instrumented flux return of the magnet allows discrimination of muons from pions.

We reconstruct $B^0 \to a_1^+\rho^-$ candidates from combinations of $a_1^+ \to \pi^+\pi^-\pi^+$ and $\rho^- \to \pi^0\pi^-$ candidates. The $a_1(1260) \to 3\pi$ decay proceeds mainly through the intermediate states $(\pi\pi)_\rho\pi$ and $(\pi\pi)_\sigma\pi$ [12]. We do not distinguish between the dominant P-wave $(\pi\pi)_\rho$ and S-wave $(\pi\pi)_\sigma$ in the channel $\pi^+\pi^-$. The Monte Carlo (MC) signal events are simulated as B^0 decays to $a_1^+(1260)\rho^-$ with $a_1^+ \to \rho^0\pi^+$ using the GEANT4-based [13] *BABAR* MC simulation. Possible contributions from B^0 decays to $a_2^+(1320)\rho^-$ and $\pi^+(1300)\rho^-$ are investigated.

We only consider events that have a minimum of one π^0 and four charged tracks, where the charged tracks are required to be inconsistent with lepton, proton and kaon hypotheses.

We form $\pi^0 \to \gamma\gamma$ candidates from pairs of photon candidates that have been identified as localized energy deposits in the EMC that have the lateral energy distribution expected for a photon. Each photon is required to have an energy $E_\gamma > 50\,\mathrm{MeV}$, and the π^0 is required to have an invariant mass of $0.10 < m_{\gamma\gamma} < 0.16\,\mathrm{GeV}/c^2$.

The ρ^- mesons are formed from one track that is consistent with a π^- and the aforementioned π^0 candidate. The candidate ρ^- is required to have an invariant mass of $0.5 < m_{\rho^-} < 1.1\,\mathrm{GeV}/c^2$. We also constrain the cosine of the angle between the π^0 momentum and the direction opposite to the B^0 in the ρ^- rest frame ($\cos\theta_{\rho^-}$) to be between -0.9 and 0.98. This removes backgrounds which peak at the extremes of the distribution where the signal reconstruction efficiency also falls off.

We form the a_1^+ candidate from combinations of three charged pions. We first form a $\rho^0 \to \pi^+\pi^-$ candidate from two oppositely charged tracks. This combination is required to have an invariant mass of $0.4 < m_{\rho^0} < 1.1\,\mathrm{GeV}/c^2$. The a_1^+ candidate is then formed by adding another charged track to the ρ^0, and requiring that the mass of the a_1^+ satisfies $0.6 < m_{a_1^+} < 1.5\,\mathrm{GeV}/c^2$. The vertex of the B-candidate is constrained to originate from the beam spot. In order to reduce background from continuum events we require that $|\cos(\theta_T)| < 0.7$, where θ_T is the angle between the B thrust axis and that of the rest of the event (ROE).

We use two kinematic variables, m_{ES} and ΔE, in order to isolate any signal. We define the beam-energy substituted mass $m_{\mathrm{ES}} = \sqrt{(\sqrt{s}/2)^2 - (p_B^*)^2}$, where $\sqrt{s}$ is the e^+e^- center-of-mass (CM) energy. The second kinematic variable, ΔE, is the difference between the B-candidate energy and the beam energy in the CM frame. We require $m_{\mathrm{ES}} > 5.25\,\mathrm{GeV}/c^2$ and $-0.15 < \Delta E < 0.1\,\mathrm{GeV}$.

Additional separation between signal and continuum is obtained by combining several kinematic and topological variables into a Fisher discriminant ($\mathcal{F}$) [14]. The variables L_0, L_2, and $|\cos\theta_{TR}|$, and the output of a multivariate tagging algorithm [15] are used as inputs to $\mathcal{F}$. L_0 and L_2 are defined as

$$L_0 = \sum_{\rm ROE} |p_i^*|,\ L_2 = \sum_{\rm ROE} |p_i^*| \cos(\theta_i)^2, \quad (1)$$

where the sum is over the ROE, p_i^* is the particle momentum in the CM frame. θ_i is the angle of the particle direction relative to the thrust axis of the B-candidate, and $\cos\theta_{TR}$ is the cosine of the angle between the B thrust axis and the beam axis. The multivariate tagging algorithm identifies the flavor of the other B in the event to be either a B^0 or $\overline{B}^0$. The output of this algorithm is ranked into categories of different signal purity.

We expect the polarization of the $a_1^+\rho^-$ final state to be predominantly longitudinal, as was found in the similar decay $B \to \rho\rho$ [4–8]. We have used both longitudinal and transverse polarized signal MC simulated data in this analysis. After applying the selection cuts above, we have 2.8 (2.3) longitudinal (transverse) polarized signal MC simulated data candidates per event.

We define as self-cross-feed (SCF) the set of candidates that were incorrectly reconstructed from particles in events that contain a true signal candidate. We select one B candidate per event in which the mass of the reconstructed ρ^0 is closest to that of the true ρ^0 mass [16]. Choosing the candidate using the ρ^0 mass reduces the SCF fraction by 18% relative to a random selection. To avoid potentially biasing our final result, we do not use information from the ρ^0 meson in the remainder of the analysis. After all selection cuts have been applied, the longitudinal and transverse signal SCF fractions are 0.58 and 0.42, respectively. The selection efficiency of longitudinal (transverse) signal is 9.44% (10.15%).

Besides the continuum background we also have background from B decays. We divide the B-background into the following four categories according to B-meson charge and the charm content of the final states: (i) $B^0 \to$ charm, (ii) $B^0 \to$ charmless, (iii) $B^\pm \to$ charm and (iv) $B^\pm \to$ charmless. From large samples of inclusive MC simulated data we expect 2394, 424, 3281 and 215 events of these background types, respectively. In addition, a number of exclusive B-background modes that have a similar final state to the signal were studied. This includes those that have an intermediate a_1 meson in the decay. None of these modes were seen to have a significant efficiency after the selection cuts had been applied.

We perform an extended unbinned maximum likelihood fit to the data. The likelihood model has the following types: (i)-(iv) the four aforementioned inclusive B-background categories, (v) true signal, (vi) SCF signal and the (vii) $e^+e^- \to q\overline{q}$ ($q = u,d,s,c$) continuum background. The probability density function (PDF) for each event i has the form $P_{i,c} = P_{i,c}(m_{\rm ES}, \Delta E, \mathcal{F}, m_{a_1^+}, m_{\rho^-}, \cos\theta_{\rho^-})$. From these individual PDFs the total likelihood

$$\mathrm{L} = e^{-n'} \prod_{i=1}^{n} \sum_{c} N_c P_{i,c}, \quad (2)$$

is constructed. The parameters n and n' are the numbers of selected on-peak events, and the sum of the yields N_c, where c is one of the seven types in the likelihood model. Correlations between the m_{ρ^-} and $\cos\theta_{\rho^-}$ variables are taken into account for the real (T) and fake combinatorial (F) ρ^- candidates. All other correlations between fit variables are seen to be small. However, the effect of ignoring them results in a bias on the fitted signal yield which is discussed below.

Each of the signal distributions has a signal yield and a polarization fraction that are denoted by N_{sig} (N'_{sig}) and f_L (f'_L), for the true (SCF) signal, such that the sum of the true and SCF signal is described by

$$N_{sig}[f_L P_i^{long,true} + (1-f_L) P_i^{tran,true}] + N'_{sig}[f'_L P_i^{long,SCF} + (1-f'_L) P_i^{tran,\ SCF}]. \quad (3)$$

The continuum yield, N_{sig}, N'_{sig}, and the parameters of the continuum $m_{\rm ES}$ and ΔE PDFs are allowed to vary in the fit. Under the assumption that no significant signal is observed, the value of f_L is fixed to 1.0 in the fit. The value of f'_L is also fixed to 1.0 in the fit since it is highly correlated with N_{sig}, N'_{sig} and f_L. Only the fitted value of N_{sig} is used to derive the final result. We also fix the B-background yields to the aforementioned values.

The PDFs used for each component are given in Table I. The signal and B-backgrounds are parameterized using MC. We use a non-parametric smoothing algorithm [17] when defining some of the background PDFs (as indicated by the abbreviation NP). We account for the difference between F and T $\rho^- \to \pi^-\pi^0$ distributions in the background using the product of 1D PDFs, denoted in Table I as 'BG m-hel', such that

$$P_i(m_{\rho^-}, \cos\theta_{\rho^-}) = (1-a_T) P_{F,i}(m_{\rho^-}) P_{F,i}(\cos\theta_{\rho^-}) + a_T P_{T,i}(m_{\rho^-}) P_{T,i}(\cos\theta_{\rho^-}), \quad (4)$$

where a_T is the fraction of T events. The continuum shape for $\cos\theta_{\rho^-}$ (m_{ρ^-}) is derived from off-peak (on-peak) data. The true ρ^- resonance Breit Wigner shape uses $m_{\rho^-} = 0.77$ GeV/c^2, and $\Gamma = 0.150$ GeV [16]. The parameterizations used for this PDF are summarized in Table II.

The results from the fit are $N_{sig} = 90 \pm 38$(stat), $N'_{sig} = 42 \pm 98$ and a continuum yield of 25798 ± 182 events. The bias on the fitted signal yield is evaluated by performing ensembles of mock experiments using signal MC embedded into MC samples of background generated from

TABLE I: The types of PDFs used to model the different variables for each component in the likelihood fit, where the PDFs underlined have their parameters varying in the nominal fit. The abbreviations are: G = Gaussian, G2 = Double Gaussian, G3 = Triple Gaussian, CB = Crystal Ball (a Gaussian with a low side exponential tail) [18], ARGUS = ARGUS function $x\sqrt{1-x^2}\exp\left[-\xi(1-x^2)\right]$, with $x \equiv 2m_{\rm ES}/\sqrt{s}$ and parameter ξ [19], which is allowed to vary in the fit, Pn = Polynomial of order n, BW = Breit-Wigner, helicity = $\cos^2\theta_{\rho^-}$ or $\sin^2\theta_{\rho^-}$ depending on partial wave which is modified by a quadratic acceptance function, BG m-hel = Background $\cos\theta_{\rho^-}$ and m_{ρ}^- PDF of Eq. 4, off-peak = PDF taken from off-peak data, and 1D = smoothed 1D histogram.

Component	$m_{\rm ES}$	ΔE	$\mathcal{F}$	$m_{a_1^+}$	$\cos\theta_{\rho^-}$	m_{ρ^-}
signal (long/trans./true/SCF)	CB	CB+G	G2	G3	helicity	BW+P4
$q\overline{q}$	<u>ARGUS</u>	<u>P1</u>	G2 (off-peak)	1D (off-peak)	BG m-hel	BG m-hel
B^0 ($B^{\pm}$)$\rightarrow$ charm (charmless)	NP	NP	NP	NP	BG m-hel	BG m-hel

TABLE II: The types of PDFs used to model the different background $\cos\theta_{\rho^-}$ and m_{ρ^-} PDF shapes. The abbreviations Pn and BW are defined in the caption of Table I.

Component	T $\cos\theta_{\rho^-}$	T m_{ρ^-}	F $\cos\theta_{\rho^-}$	F m_{ρ^-}
$q\overline{q}$	P2	BW + P1	P5	P4
$B^{\pm}\rightarrow$ charmless	P4	BW	P5	P3
$B^0\rightarrow$ charmless	P4	BW	P5	P3
$B^{\pm}\rightarrow$ charm	P2	BW	P5	P3
$B^0\rightarrow$ charm	P2	BW	P5	P3

the PDF. The bias is found to be +22 events (24%), resulting in a corrected signal yield of 68 ± 38(stat). In Fig. 1 we compare the true signal and continuum PDF shapes (solid curves) to the data (points) using the event-weighting technique described in Ref. [20]. The distributions shown in Fig. 1 are not corrected for fit bias, and the uncertainty on each of the data points is statistical. No change in signal yield is seen when $a_2^+(1320)\rho^-$ and $\pi^+(1300)\rho^-$ components are included in the fit.

Table III summarises the systematic uncertainties on the signal yield. Each entry in the table indicates one systematic effect, and the contributions are added in quadrature to give the total presented. The uncertainty due to PDF parameterisation is evaluated by variation of both the signal and the background PDF parameters within their uncertainties about their nominal values. The uncertainty from the continuum $m_{\rm ES}$ and ΔE PDFs which are allowed to vary in the fit, are only included in the quoted statistical uncertainty. We assign a systematic uncertainty due to fit bias, evaluated as half of the fit bias correction on the signal yield. To validate the expected B-background yields, and to assign a systematic uncertainty we perform a number of cross-checks in which we allow the background yields to vary in turn when fitting the data. We use a control sample of $B\rightarrow D\rho$ events to determine the systematic uncertainty in the fraction of SCF signal events. The effect of exclusive B meson decays to final states including a_1-mesons were evaluated using ensembles of mock experiments. In particular, the systematic uncertainty on the signal yield from neglecting $B\rightarrow a_1a_1$ modes in the fit is 6 events. We assign a systematic uncertainty from using a relativistic Breit-Wigner with a Blatt-Weisskopf form factor with a range parameter of 3.0 GeV^{-1} for the a_1^+ meson line shape. In the fit we assume that the a_1^+ meson width, $\Gamma_{a_1^+}$, is 400 MeV. We evaluate a systematic uncertainty due to this assumption by varying $\Gamma_{a_1^+}$ over the experimentally allowed range: 250 - 600 MeV [16]. The difference in the distribution of $\mathcal{F}$ between data and MC is evaluated with a large sample of $B\rightarrow D^{\star}\rho$ decays. The systematic uncertainties that contribute to the branching fraction only through the efficiency come from charged particle identification (6.0%), π^0 meson reconstruction (3.0%), tracking efficiency (3.2%), and the number of B meson pairs (1.1%). The systematic error contribution from MC statistics is negligible.

TABLE III: The systematic uncertainties on N_{sig} (events).

Source	Uncertainty on N_{sig}
PDF parameterisation	$^{+27}_{-30}$
Fit bias	± 11
B-background yields	$^{+29}_{-42}$
SCF fraction	± 7
Neglecting $B\rightarrow a_1a_1$ modes in fit	± 6
a_1^+ line shape	± 10
a_1^+ width	± 9
Fisher data/MC comparison	± 6
Total	$^{+45}_{-56}$

When the fit bias correction of -22 events is applied to the signal yield, and one accounts for systematic uncertainties, the significance of the result is

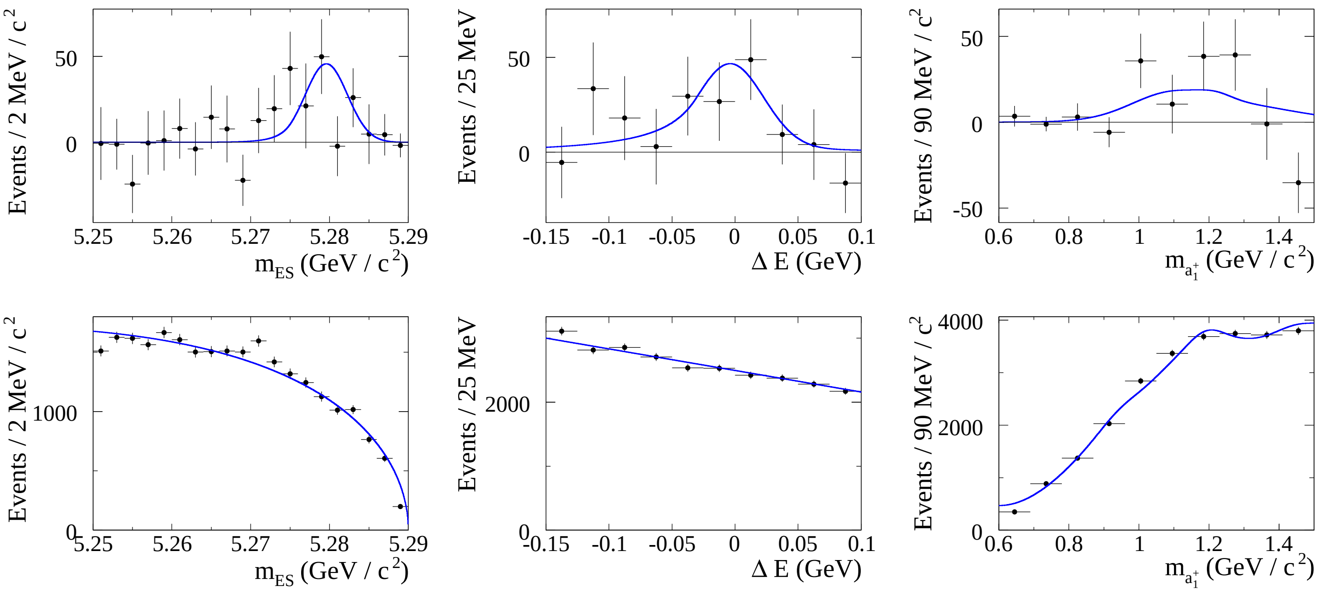

FIG. 1: The true signal (top) and continuum (bottom) distributions for (left to right) $m_{\rm ES}$, ΔE, $m_{a_1^+}$ using the weighting technique described in Ref. [20]. The points represent the weighted data, and solid curves represent the corresponding PDFs.

0.95 standard deviations. Figure 2 shows the distribution of $-\ln(\mathrm{L}/\mathrm{L}_{\max})$ for the fit, with and without these systematic errors. $\mathrm{L}_{\max}$ is the value of the likelihood corresponding to the nominal fit result. The branching fraction value for the fit-bias-corrected signal yield of $68 \pm 38(\mathrm{stat})^{+45}_{-56}(\mathrm{syst})$ is $\mathcal{B}(B^0 \to a_1^+\rho^-)\mathcal{B}(a_1^+ \to \pi^+\pi^-\pi^+) = (15.7 \pm 8.7(\mathrm{stat})^{+10.3}_{-12.8}(\mathrm{syst}))\times 10^{-6}$. This assumes that $f_L = 1.0$ and that the branching fraction of $a_1^+ \to \pi^+\pi^-\pi^+ = 0.5$. As the signal yield obtained is not significant, we calculate the upper limit $x_{\rm UL}$, by

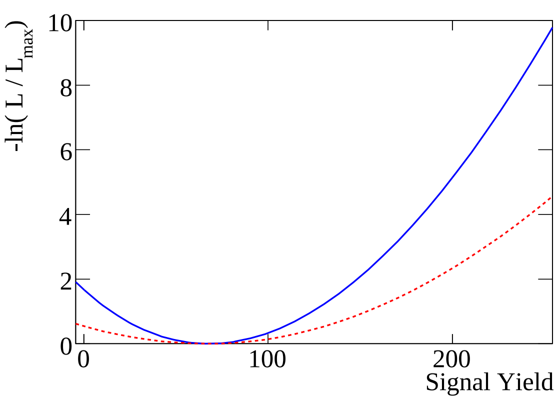

FIG. 2: The $-\ln(\mathrm{L}/\mathrm{L}_{\max})$ distribution from the fit to data with f_L=1.0 (fixed). This distribution has been corrected for fit bias. The solid curve is for statistical errors only, and the dashed curve includes systematic errors.

integrating the likelihood function (including systematic uncertainties) from 0 to $x_{\rm UL}$, for different physically allowed values of f_L, such that the C.L. of the upper limit is 90%. As the signal efficiency is a function of f_L, we report the most conservative upper limit obtained, which corresponds to $f_L = 1.0$. On doing this, an upper limit of 30×10^{-6} (90% C.L.) is obtained.

We have performed a search for the decay $B^0 \to a_1^\pm\rho^\mp$ in a data sample of 100 fb^{-1}. After correcting for fit bias and accounting for systematic uncertainties, the signal yield is $68 \pm 38(\mathrm{stat})^{+45}_{-56}(\mathrm{syst})$ events, with a significance of 0.95σ. As there is no significant evidence for a signal, we place an upper limit of 30×10^{-6} (90% C.L.) on $\mathcal{B}(B^0 \to a_1^+\rho^-)\mathcal{B}(a_1^+ \to \pi^+\pi^-\pi^+)$, where we assume that the a_1^+ decays exclusively to $\rho^0\pi^+$. Assuming $\mathcal{B}(a_1^+ \to \pi^+\pi^-\pi^+)$ is equal to $\mathcal{B}(a_1^+ \to \pi^+\pi^0\pi^0)$, we obtain $\mathcal{B}(B^0 \to a_1^+\rho^-)\mathcal{B}(a_1^+ \to (3\pi)^+) < 61\times10^{-6}$ (90% C.L.). This upper limit corresponds to a significant improvement over the previous bound and is compatible with theoretical expectations [10]. This result is a significant improvement in constraining an important B background contribution in $B \to \rho\rho$ decays.

ACKNOWLEDGMENTS

We are grateful for the excellent luminosity and machine conditions provided by our PEP-II colleagues, and for the substantial dedicated effort from the computing organizations that support *BABAR*. The collaborating institutions wish to thank SLAC for its support and kind hospitality. This work is supported by DOE and NSF (USA), NSERC (Canada), IHEP (China), CEA and CNRS-IN2P3 (France), BMBF and DFG (Germany), INFN (Italy), FOM (The Netherlands), NFR (Norway), MIST (Russia), and PPARC (United Kingdom). Individuals have received support from CONACyT (Mexico), Marie Curie EIF (European Union), the A. P. Sloan Foundation, the Research Corporation, and the Alexander von Humboldt Foundation.

* Also at Laboratoire de Physique Corpusculaire, Clermont-Ferrand, France
† Also with Università di Perugia, Dipartimento di Fisica, Perugia, Italy
‡ Also with Università della Basilicata, Potenza, Italy

[1] N. Cabibbo, Phys. Rev. Lett. **10**, 531 (1963); M. Kobayashi and T. Maskawa, Prog. Theor. Phys. **49**, 652 (1973).
[2] Charge-conjugate transitions are included implicitly unless otherwise stated.
[3] A. Bevan, Mod. Phys. Lett. A **21**, No. 4, 305 (2006).
[4] The *BABAR* Collaboration, B. Aubert *et al.*, Phys. Rev. Lett. **95**, 041805 (2005).
[5] The *BABAR* Collaboration, B. Aubert *et al.*, Phys. Rev. Lett. **91**, 171802 (2003).
[6] The *BABAR* Collaboration, B. Aubert *et al.*, Phys. Rev. Lett. **94**, 131801 (2005).
[7] The Belle Collaboration, A. Somov *et al.*, arXiv:hep-ex/0601024. Submitted to PRL.
[8] The Belle Collaboration, J. Zhang *et al.*, Phys. Rev. Lett. **91**, 221801 (2003).
[9] The ARGUS Collaboration, H. Albrecht *et al.*, Phys. Lett. B **241**, 278 (1990).
[10] M. Bauer, B. Stech and M. Wirbel, Z. Phys. C **34**, 103 (1987).
[11] The *BABAR* Collaboration, B. Aubert *et al.*, Nucl. Instr. Methods Phys. Res., Sect. A **479**, 1 (2002).
[12] The CLEO Collaboration, D. M. Asner *et al.*, Phys. Rev. D **61**, 012002 (1999).
[13] The GEANT4 Collaboration, S. Agostinelli *et al.*, Nucl. Instr. Methods Phys. Res., Sect. A **506**, 250 (2003).
[14] R. A. Fisher, Annals of Eugenics 7, 179 (1936).
[15] The *BABAR* Collaboration, B. Aubert *et al.*, Phys. Rev. Lett. **89**, 281802 (2002).
[16] S. Eidelman *et al.*, Phys. Lett. B **592**, 1 (2004).
[17] K. S. Cranmer, Comput. Phys. Commun. **136**, 198 (2001).
[18] The Crystal Ball Collaboration, D. Antreasyan *et al.*, Crystal Ball Note, 321 (1983).
[19] The ARGUS Collaboration, H. Albrecht *et al.*, Phys. Lett. B **241**, 278 (1990).
[20] M. Pivk and F. R. Le Diberder, Nucl. Instr. Methods Phys. Res., Sect. A **555**, 356 (2005).